Dielectric properties of nucleated erythrocytes as simulated by the double spherical-shell model

Jia Xu(徐佳)[1], Weizhen Xie(谢伟珍)[1], Yiyong Chen(陈一勇)[1], Lihong Wang(王立洪)[2], and Qing Ma(马青)[1,†]

Citation: Chin. Phys. B, 2020, 29 (**12**): 128703. DOI: 10.1088/1674-1056/abbbf0
Journal homepage: http://cpb.iphy.ac.cn; http://iopscience.iop.org/cpb

What follows is a list of articles you may be interested in

Optoelectronic memristor for neuromorphic computing

Wuhong Xue(薛武红), Wenjuan Ci(次文娟), Xiao-Hong Xu(许小红), Gang Liu(刘钢)
Chin. Phys. B, 2020, 29 (**4**): 048401. DOI: 10.1088/1674-1056/ab75da

Effects of bismuth on structural and dielectric properties of cobalt-cadmium spinel ferrites fabricated via micro-emulsion route

Furhaj Ahmed Sheikh, Muhammad Khalid, Muhammad Shahzad Shifa, H M Noor ul Huda Khan Asghar, Sameen Aslam, Ayesha Perveen, Jalil ur Rehman, Muhammad Azhar Khan, Zaheer Abbas Gilani
Chin. Phys. B, 2019, 28 (**8**): 088701. DOI: 10.1088/1674-1056/28/8/088701

Effects of Shannon entropy and electric field on polaron in RbCl triangular quantum dot

M Tiotsop, A J Fotue, S C Kenfack, N Issofa, H Fotsin, L C Fai
Chin. Phys. B, 2016, 25 (**4**): 048401. DOI: 10.1088/1674-1056/25/4/048401

Effects of A1 site occupation on dielectric and ferroelectric properties of $Sr_4CaRTi_3Nb_7O_{30}$ (R=Ce, Eu) tungsten bronze ceramics

Fang Yu-Jiao, Gong Gao-Shang, Gebru Zerihun, Yuan Song-Liu
Chin. Phys. B, 2014, 23 (**12**): 128701. DOI: 10.1088/1674-1056/23/12/128701

Analysis and modeling of resistive switching mechanism oriented to fault tolerance of resistive memory based on memristor

Huang Da, Wu Jun-Jie, Tang Yu-Hua
Chin. Phys. B, 2014, 23 (**3**): 038404. DOI: 10.1088/1674-1056/23/3/038404

Dielectric properties of nucleated erythrocytes as simulated by the double spherical-shell model*

Jia Xu(徐佳)[1], Weizhen Xie(谢伟珍)[1], Yiyong Chen(陈一勇)[1], Lihong Wang(王立洪)[2], and Qing Ma(马青)[1,†]

[1] School of Medicine, Ningbo University, Ningbo 315211, China
[2] School of Mathematics and Statistics, Ningbo University, Ningbo 315211, China

(Received 23 July 2020; revised manuscript received 16 September 2020; accepted manuscript online 28 September 2020)

The dielectric properties of nucleated erythrocytes from bullfrogs were measured in a frequency range of 10 kHz–110 MHz. The complex permittivity (ε^*), complex conductivity (κ^*), and complex resistivity (ρ^*) were analyzed and compared in the 10.63% to 37.58% haematocrit (Hct) range. The relaxation behavior, the passive electrical properties, and the cellular structure parameters, including the cell membrane, the cytoplasm, the nuclear membrane, and the nucleoplasm of the nucleated erythrocyte suspensions were investigated. The method used is based on the binomial Cole–Cole equation and the double spherical-shell physical models. Upon the elimination of the electrode polarization effect, two definite relaxations related to the interfacial polarization are observed on low- and high-frequency dispersions. The permittivity values and the characteristic frequency values differ by one order of magnitude: the low-frequency relaxation increments [$\Delta\varepsilon_1 = (5.63 \pm 1.43) \times 10^3$] and the characteristic frequency [$f_{c1} = (297.06 \pm 14.48)$ kHz] derived from the cell membrane, the high-frequency relaxation increments [$\Delta\varepsilon_2 = (5.21 \pm 1.20) \times 10^2$] and the characteristic frequency [$f_{c2} = (3.73 \pm 0.06)$ MHz] derived from the dielectric response to the external electric field of the nuclear membrane, respectively. Moreover, the other core dielectric parameters, such as the relative permittivity of the cell membrane [$\varepsilon_m = (7.57 \pm 0.38)$] and the nuclear envelope [$\varepsilon_{ne} = (23.59 \pm 4.39)$], the conductivity of the cytoplasm (hemoglobin, $\kappa_{Hb} = (0.50 \pm 0.13)$ S/m] and the nuclear endoplasm [$\kappa_{np} = (2.56 \pm 0.75)$ S/m], and the capacitance of the bilayer membranes [C_m: (0.84 ± 0.04) μF/cm^2], and C_{ne}: (0.52 ± 0.10) μF/cm^2] were also accurately and reliably measured. This work presents a feasible method to evaluate the dielectric parameters and the cellular structure of the erythrocytes of bullfrogs. Moreover, it paves the way for new studies on the haematology of frogs and the detection of nucleated cells via dielectric impedance spectroscopy.

Keywords: dielectric impedance spectroscopy, bullfrog erythrocytes, the double spherical-shell model, passive electrical property

PACS: 87.19.rf, 84.37.+q **DOI:** 10.1088/1674-1056/abbbf0

1. Introduction

The dielectric properties of blood mainly depend on the electrical properties of its plasma and mature erythrocytes.[1] Mapping the evolution of these properties can be used for clinically diagnosing anaemia, coagulation pathologies, thrombosis, and malaria. The effective permittivity, conductivity, and resistivity parameters of the erythrocytes are the basis of both the analysis and interpretation of the blood thermal conductivity, magnetic permeability, diffusion coefficient, and dielectric relaxation phenomena.[2] In particular, the dielectric properties of erythrocytes are of great clinical significance to understand the dielectric hemagglutination reaction (RIHA) as well as radiofrequency and microwave hyperthermia, to perform non-invasive measurements of the cardiac output, and to predict the risk of venous thrombosis.[3] Although the dielectric properties of erythrocytes have been extensively investigated, the structural and dielectric properties of erythrocytes obtained from different biological sources are still unclear. Investigating the core parameters of bullfrogs' nucleated erythrocytes may enrich the erythrocytes' biological sources, and provide more comprehensive information in understanding their dielectric properties. In a previous study by this research group,[4] the Cole–Cole parameters [the relative permittivity at high frequency (ε_h), the first and the second relative permittivity increments ($\Delta\varepsilon_1$, $\Delta\varepsilon_2$), the first and the second characteristic frequencies (f_{c1}, f_{c2}), the first and the second phase angles (β_1, β_2), and the low-frequency conductivity (κ_l)] which describe the dielectric properties of the nucleated erythrocytes of bullfrogs were identified. Furthermore, the permittivity, conductivity, and resistivity spectra parameters, together with the dielectric parameters of the bullfrog-erythrocytes, were defined based on the double spherical-shell model.

Dielectric spectroscopy in biological systems has been

*Project supported by the National Natural Science Foundation of China (Grant Nos. 51277099 and 52007087), the Natural Science Foundation of Zhejiang Province, China (Grant Nos. LY20C110001 and LSY19A010002), the Natural Science Foundation of Ningbo City, China (Grant Nos. 2019A610349 and 202003N4116), the Fund from the Educational Commission of Zhejiang Province, China (Grant No. Y202044047), and the Fundamental Research Funds for the Provincial Universities of Zhejiang Province, China.

†Corresponding author. E-mail: maqing@nbu.edu.cn

proven to be a powerful tool to investigate blood systems via different cell-impedance measurement technologies, which are sensitive, fast, non-invasive, and available in a broad frequency range. The blood tissue mostly contains blood cells and plasma proteins. Moreover, it is a complex system with dielectric response over a broad frequency range including radio frequencies (RFs), microwaves (MWs), and near-infrared (NIR) light. Exploring the structure and the overall conductivity of the blood cells obtained from various biological sources is of pivotal importance in providing pathological diagnoses and in classifying several aspects of the human biological evolution and genetics. Bielinska[5] compared the dielectric, haematological, and biochemical characteristics of the blood of the *Cyprinus carpio* fish upon its exposure to sublethal doses of sodium alkyl benzene sulfonate (SDBS) with the blood obtained from a control group. The results show that the dielectric parameters can be correlated with the haematological parameters, but not with the biochemical ones. A variation in the haematocrit of the nucleated red blood cells (RBC) of the fish induces a change in the maximum of the dielectric loss factor ($\tan\delta$). The increase in the electrical conductivity and permittivity of the RBC may be related to the decrease in the mean corpuscular haemoglobin.[5] In order to investigate the effect of the nucleus on the dielectric behavior of the whole cell, Asami *et al*. compared and analyzed the permittivity and conductivity of lymphocytes and erythrocytes of mice in the frequency range of 0.1 MHz–250 MHz. They proposed the use of single-shell and double spherical-shell models to analyze the importance of non-nucleated RBC and nucleated lymphocytes, respectively.[6] Asami prepared cell pellets from a horse erythrocyte suspension via centrifugation; the samples were subjected to a series of intense AC pulses and characterized via cell electrofusion and dielectric spectroscopy in the frequency range of 10 Hz–10 MHz. Moreover, Asami measured the conductivity of the cell pellets (0.5 S/m) by using a curve fitting model, and identified the effects of the volume fraction and the cell radius on the low-frequency dielectric relaxation increment and the low-frequency characteristic frequency.[7] Gimsa *et al.* used dielectric electrophoresis (DEP), electrorotation (ROT), and several other electrical orientation techniques to explore the dielectric properties of the nucleated RBC. The results show that the relative permittivity of the chicken-RBC cytoplasm is in the range of 35–45, whereas the conductivity is in the range of 0.36 S/m–0.04 S/m. The cell membrane has a specific conductivity of 3500 S/m^2 and a capacitance of 10 mF/m^2–14 mF/m^2.[8] In recent years, David *et al*. measured the low-frequency dielectric relaxation increment of fresh and blood-bank cold storage RBC (188.9 and 176.0, respectively) via time domain dielectric spectroscopy (TDDS) in the frequency range of 500 kHz–1 GHz. The results provide an important reference basis to assess the quality of the tests on refrigerated human blood.[9] The studies on the dielectric properties have enriched the understanding of the cellular structure, relaxation phenomena, and differential expression of the erythrocytes obtained from various biological sources. However, the internal structural parameters and the dielectric properties of nucleated erythrocytes of bullfrogs have not been reported yet.

In this paper, the permittivity, conductivity, and resistivity spectra of the erythrocytes of the bullfrog (*Rana catesbeiana*) were obtained via dielectric impedance spectroscopy. Moreover, the dielectric properties of the erythrocyte membrane, cytoplasm, nuclear membrane, and nucleoplasm were investigated by using the Cole–Cole and the double spherical-shell physical models. The results provide an effective analysis tool and support the data collection, the parameter extraction methods, and the electrical characteristics analysis of nucleated erythrocytes. This work provides a monitoring method to investigate the properties of blood from various biological sources.

2. Materials and methods

2.1. Preparation of the bullfrog erythrocytes

Bullfrogs (*Rana catesbiana*) with 0.3 kg–0.4 kg weight of both sexes were purchased from the Ningbo University vegetable market. A metal probe was used to damage the bullfrogs' brain and spinal cord. The bullfrogs were immobilized and the blood from their aorta was collected in several EDTA-K2 vacuum blood collection vessels. The blood was centrifuged at room temperature (25 °C) in a 5430R centrifuge (Eppendorf, Gemany) at 3000 rpm for 15 min to remove the upper plasma layer and the buffy coat (leukocytes and platelets). Only the lower layer (erythrocytes) was retained. The erythrocytes were washed with a Ringer's solution for 3 times and concentrated by centrifugation. The samples were then diluted with the Ringer's solution and suspensions with different haematocrit contents were obtained (Hct). They were left resting for 1 h to equilibrate and then measured via impedance spectroscopy.

2.2. Dielectric measurements

The dielectric impedance spectra of the bullfrog erythrocytes were obtained by using a 4294A precision impedance analyser (Agilent, Japan), a 42942A adapter, a 16092 fixture, and a sample measurement cell. The sample measuring cell (Fig. 1) was a Plexiglas round tube with an inner diameter of 3.16 mm, a length of 9.35 mm, and with parallel platinum plates (Pt electrodes) fixed at both ends. Two channels were placed in the middle of the tube and used to inject the red blood

cell suspension. The volume of the measuring cell was about 75 μL.

A KCl standard solution (0.1 mol·L^{-1}) was used for calibration at 25 °C. The cell constant (C_0) is 0.00785 pF, the stray capacitance (C_1) is 2.10 pF, and the residual inductance (L) is 2.00 nH. In the 40 Hz–110 MHz range, the capacitance (C) and conductance (G) were measured with 200 frequency points by using the logarithmic mode of the C–G parallel measurement. Each sample was measured within 60 seconds under an AC excitation voltage of 100 mV. In order to reduce the deviation caused by the inductance effect of the electrode in the high frequency band, the C and G values were corrected by using the following expressions:[10]

$$\text{corrected capacitance: } C_s = \frac{C\left(1+\omega^2 LC\right)+LG^2}{\left(1+\omega^2 LG\right)^2+\left(\omega LG\right)^2} - C_1, \quad (1)$$

$$\text{corrected conductance: } G_s = \frac{G}{\left(1+\omega^2 LG\right)^2+\left(\omega LG\right)^2}, \quad (2)$$

here, ω is the angular frequency ($\omega = 2\pi f$), f is the electric field frequency, ε is the permittivity ($\varepsilon = C_s/C_0$), κ is the conductivity ($\kappa = G_s \times \varepsilon_v/C_0$), ρ is the resistivity ($\rho = 1/\kappa$), and ε_v is the vacuum permittivity ($\varepsilon_v = 8.8541$ pF/m).

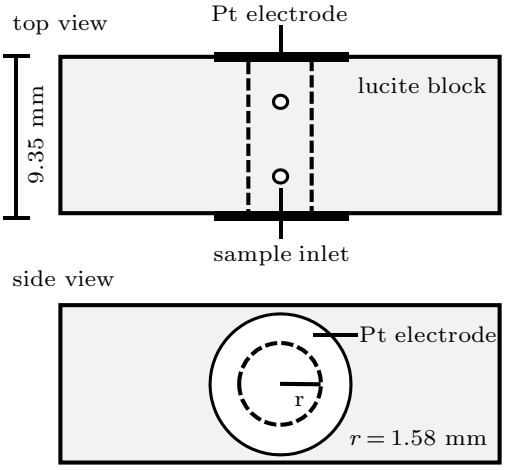

Fig. 1. Diagram of parallel plate capacitor measurement cell.

2.3. Cole–Cole mathematical model parameter analysis

Under the effect of an applied electric field, nucleated erythrocytes show a dispersion of their interface polarization, which corresponds to the dispersion behavior of the dielectric constant and the loss. In the 10 kHz–110 MHz frequency range, the dielectric response of the nucleated erythrocytes presents two relaxation processes, which are mainly driven by the β dispersion as reported in previous literature.[4,11] In order to clarify the dielectric contribution in each part of the cellular structure, such as the cell membrane, the cytoplasm, the nuclear membrane, and the nucleoplasm, the Cole–Cole mathematical model was used to extract the dielectric impedance spectrum parameters.[12–16] Equation (3) contains a negative m power (Af^{-m}) term, which reflects the polarization of the electrode,

$$\varepsilon^* = \varepsilon_h + \frac{\kappa_l}{j2\pi f\varepsilon_v} + \frac{\Delta\varepsilon_1}{1+(jf/f_{c1})^{\beta_1}} + \frac{\Delta\varepsilon_2}{1+(jf/f_{c2})^{\beta_2}} + Af^{-m}, \quad (3)$$

here, ε^* is the complex permittivity

$$\varepsilon^* = \varepsilon - j[\kappa/(\omega\times\varepsilon_v)] = \varepsilon - j[\varepsilon'' + \kappa_l/(\omega\times\varepsilon_v)],$$

where j is the unit of the imaginary part ($j = \sqrt{-1}$), κ_l is the limiting conductivity at low frequencies, ε_h is the permittivity at high frequencies, ε'' is the dielectric loss ($\varepsilon'' = \kappa - \kappa_l/(\omega\times\varepsilon_v)$), and κ'' is the imaginary part of the conductivity ($\kappa'' = \varepsilon_v \times \omega \times (\varepsilon - \varepsilon_h)$). $\Delta\varepsilon_1$, $\Delta\varepsilon_2$, f_{c1}, f_{c2}, and β_1, β_2 represent the low- and high-frequency relaxation increments, the characteristic frequencies, and the Cole–Cole parameters ($0 < \beta \le 1$), respectively.

2.4. Double spherical-shell physical model analysis

The morphological characteristics of the bullfrog nucleated erythrocytes[17] with either an oval or a round shape and with a smooth surface were simulated as double-layer spherical shell structures with concentric centres. They exhibited nuclei, but no organelles were present in the cytoplasm. Owing to the non-uniform conductivity of the extracellular membrane, cell membrane, cytoplasm, nuclear membrane, and nucleoplasm and the action of a broadband alternating electric field, the cell suspension exhibited a strong dispersion effect (β-dispersion) similar to the inherent dipole relaxation. An effective analysis method involves considering the β-relaxation as an intrinsic relaxation process and using the equivalent circuit method[18] combined with the Maxwell–Wagner equation to obtain the electrical characteristics of the low-concentration cell suspensions.[19,20] By defining a double spherical-shell physical model (Fig. 2), the curve fitting parameters were correlated with the intrinsic dielectric properties of the different structural regions of the nucleated erythrocytes.[11] These results further clarify the contributions of the internal structures of the nucleated erythrocytes to their dispersion behavior and provide the structural parameter information on the nucleated erythrocytes.

Figure 2 shows the double spherical-shell physical model of the bullfrog nucleated erythrocytes, which were simulated as spherical particles (ε^*_{sp}) suspended in an extracellular fluid (ε^*_o) with various volume fractions (Φ, also known as haematocrit, Hct). According to the Maxwell–Wagner equation,[21] the complex permittivity (ε^*) of the whole cell suspension can be expressed via the following expression:

$$\varepsilon^* = \varepsilon^*_o \frac{2(1-\Phi)\varepsilon^*_o + (1+2\Phi)\varepsilon^*_{sp}}{(2+\Phi)\varepsilon^*_o + (1-\Phi)\varepsilon^*_{sp}}, \quad (4)$$

here, ε_{o}^{*} corresponds to the extracellular complex permittivity and ε_{sp}^{*} represents the equivalent complex permittivity of the cell particles. The ε_{sp}^{*} value consists of the contributions of the cell membrane phase (ε_{m}^{*}) and the intracellular phase (ε_{in}^{*}), as shown in Fig. 2(b). These values can be calculated according to the following formula:

$$\varepsilon_{sp}^{*}=\varepsilon_{m}^{*}\frac{2(1-\Phi_{in})\varepsilon_{m}^{*}+(1+2\Phi)\varepsilon_{in}^{*}}{(2+\Phi_{in})\varepsilon_{m}^{*}+(1-\Phi_{in})\varepsilon_{in}^{*}}, \tag{5}$$

where ε_{m}^{*} refers to the cell membrane complex permittivity, ε_{in}^{*} is the intracellular complex permittivity, and Φ_{in} is the volume fraction inside the cell. In the $\Phi_{in}=(1-d/R)^{3}$ expression, d corresponds to the cell membrane thickness, and R is the cell radius.

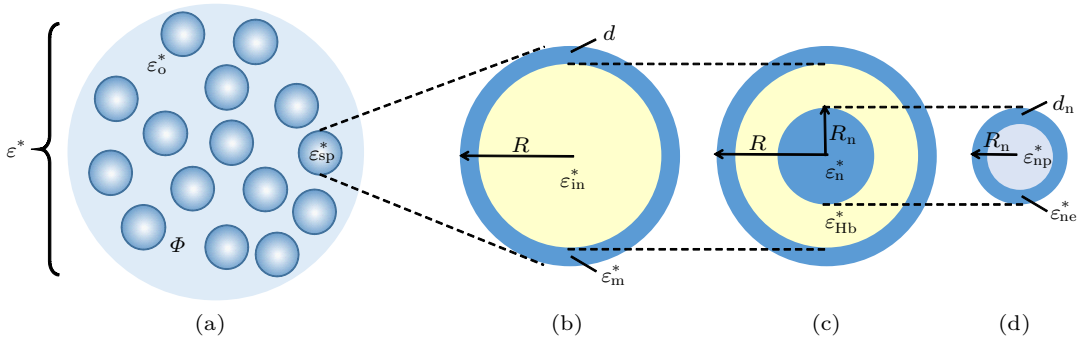

Fig. 2. Double spherical-shell physical model of the bullfrog nucleated erythrocytes and the dielectric and geometric parameters of their constituent structures (cell membrane, cytoplasm, nuclear membrane, and nucleoplasm). (a) Spherical particles (Φ) are suspended in the extracellular medium (ε_{o}^{*}). (b) Spherical particles (ε_{sp}^{*}) consisting of both the cell membrane phase (ε_{m}^{*}) and the intracellular phase (ε_{in}^{*}). (c) Intracellular phase consisting of cytoplasm (haemoglobin, ε_{Hb}^{*}) and nucleus (ε_{n}^{*}). (d) Nucleus consisting of the cell nuclear envelope (ε_{ne}^{*}) and the nucleoplasm (ε_{np}^{*}).

The value of ε_{in}^{*} can be calculated from the hemoglobin (Hb, ε_{Hb}^{*}) and the nuclear (n, ε_{n}^{*}) phases, as shown in Fig. 2(c):

$$\varepsilon_{in}^{*}=\varepsilon_{Hb}^{*}\frac{2(1-\Phi_{n})\varepsilon_{Hb}^{*}+(1+2\Phi_{n})\varepsilon_{n}^{*}}{(2+\Phi_{n})\varepsilon_{Hb}^{*}+(1-\Phi_{n})\varepsilon_{n}^{*}}. \tag{6}$$

In Eq. (6), ε_{Hb}^{*} corresponds to the haemoglobin complex permittivity, ε_{n}^{*} is the nucleus complex permittivity, and Φ_{n} is the volume fraction of the nucleus. In the expression $\Phi_{n}=[R_{n}/(R-d)]^{3}$, R_{n} refers to the radius of the nucleus.

The value of ε_{n}^{*} can be calculated from the nuclear envelope (ne, ε_{ne}^{*}) and nucleoplasm (np, ε_{np}^{*}) phases, as reported in Fig. 2(d):

$$\varepsilon_{n}^{*}=\varepsilon_{ne}^{*}\frac{2(1-\Phi_{np})\varepsilon_{ne}^{*}+(1+2\Phi_{np})\varepsilon_{np}^{*}}{(2+\Phi_{np})\varepsilon_{ne}^{*}+(1-\Phi_{np})\varepsilon_{np}^{*}}. \tag{7}$$

In Eq. (7), ε_{ne}^{*} corresponds to the nuclear membrane complex permittivity, ε_{np}^{*} is the complex permittivity inside the nucleus, and Φ_{np} is the volume fraction of the nucleoplasm. In the expression $\Phi_{np}=(1-d_{n}/R_{n})^{3}$, d_{n} refers to the thickness of the nuclear membrane.[22]

2.5. Residual analysis of curve fitting

In order to minimize the residual error between the measured data and the simulated values calculated from Eq. (3) to Eq. (4), the nonlinear least square method was used for optimization purposes. The residual sum of squares is defined as follows:[23]

$$R(\varepsilon+\kappa)=\sqrt{\sum_{i}\left(1-\frac{\log\varepsilon_{t,i}}{\log\varepsilon_{m,i}}\right)^{2}+\sum_{i}\left(1-\frac{\kappa_{t,i}}{\kappa_{m,i}}\right)^{2}}, \tag{8}$$

here t, m, and i represent the theoretical value, the measured value, and one of the frequency points, respectively. The curve-fitting parameters and the residual values of the Cole–Cole equation and the double spherical-shell model are listed in Tables 1 and 2, respectively.

3. Results

3.1. Dielectric spectra of the bullfrog erythrocytes suspension

The permittivity spectra of 17 bullfrog erythrocytes suspensions are presented in Fig. 3(a). The data shows that the permittivity (ε) gradually decreases with increase in the electric field frequency (f). The limiting low- and high-frequency values are $\varepsilon_{l}=\varepsilon|_{f=77\ \mathrm{kHz}}$ and $\varepsilon_{h}=\varepsilon|_{f=95\ \mathrm{MHz}}$, respectively. With the increase in Hct value, ε_{l} increases, whereas ε_{h} remains almost unchanged ($\varepsilon_{h}=72.59\pm3.36$). Figure 3(a) shows that the dielectric increment ($\Delta\varepsilon=\varepsilon_{l}-\varepsilon_{h}$) has a positive correlation with the Hct value: $\Delta\varepsilon=1470.11+17117.81\,Hct$ ($r=0.99$). The data reported in Figs. 3(b)–3(d) was selected from Fig. 3(a): figure 3(b) is a three-dimensional graph, which shows the dielectric spectra of the bullfrog erythrocytes. The curves in Figs. 3(c) and 3(d) exhibit a single peak and a single semi-circular shape, respectively. The two peaks correspond to the response induced from the dielectric response of the cell membrane and the nuclear membrane to the external applied AC electric field. The corresponding low- and high-frequency characteristic frequencies, $f_{c1}=(297.06\pm14.48)$ kHz and $f_{c2}=(3.73\pm0.06)$ MHz, together with the residual value, $R(\varepsilon+\kappa)=0.38\pm0.08$ ($n=17$), in Fig. 3 were obtained by using Eqs. (3) and (8).

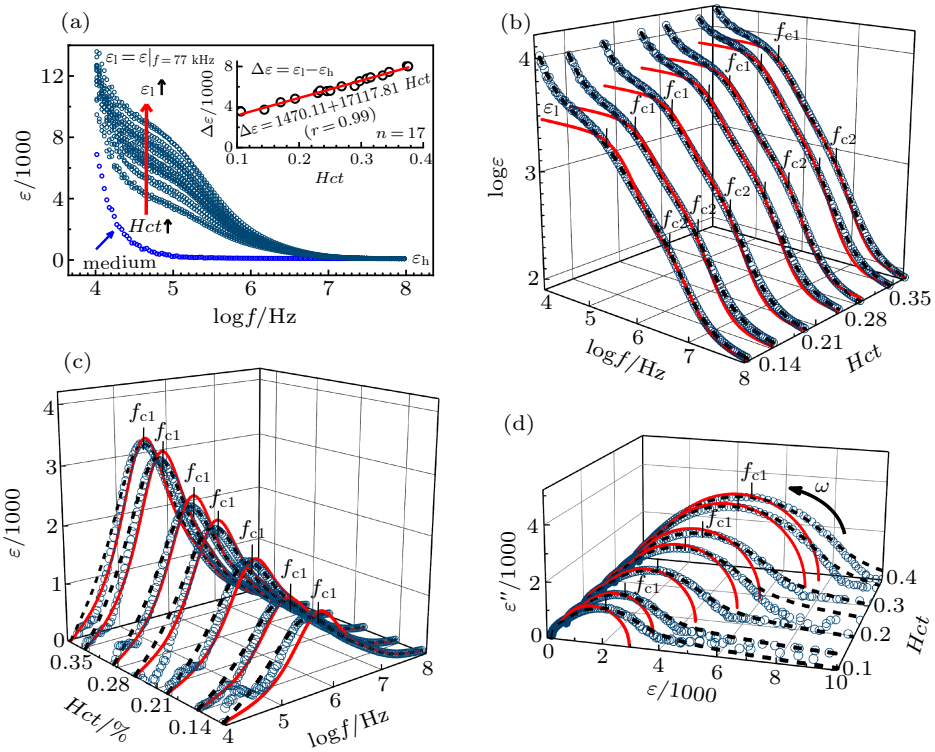

Fig. 3. Spectra of the real part [(a), (b)] and the imaginary part (c) of the complex permittivity of the bullfrog erythrocytes suspensions and its complex planes (d). The hollow circle represents the experimental data, the broken line is the Cole–Cole equation curve, and the solid line is the physical model curve based on the double spherical-shell model. Solid and broken lines denote the best-fit theoretical curves predicted from Eqs. (3)–(7). Parameters employed, as listed in Tables 1 and 2.

3.2. Conductivity spectra of the bullfrog erythrocytes suspensions

Under the condition of low extracellular conductivity (~ 0.01 S/m), the dielectric spectra are very sensitive to any change in the cell membrane conductivity.[24] Contrarily, the erythrocytes are not influenced by the electrical conductivity of the passive electric field, since the cell and the nuclear membranes are poor conductors ($\kappa_{\rm m} = 1.00 \times 10^{-7}$ S/m, $\kappa_{\rm ne} = 1.00 \times 10^{-4}$ S/m) in a highly conductive extracellular fluid [$\kappa_{\rm o} = (1.18 \pm 0.10)$ S/m]. The conductivity spectra of the bullfrog erythrocytes suspensions under different Hct values show that the erythrocyte conductivity (κ) increases with increase in the frequency (f). Its low- [$\kappa_{\rm l} = (0.77 \pm 0.11)$ S/m] and high-frequency values ($\kappa_{\rm h}$) decrease with the increase in the Hct concentration (indicated by the red arrow in Fig. 4(a)). Figure 4(a) shows that the conductivity increment ($\Delta\kappa = \kappa_{\rm h} - \kappa_{\rm l}$) has a positive linear correlation with the Hct value: $\Delta\kappa = (0.14 + 0.65)\ Hct$ ($r = 0.91$). Seven typical spectra reported in Fig. 4(a) were used to draw a three-dimensional chart of the conductivity spectra [Figs. 4(b)–4(d)]: The curves were fit via the Maxwell–Wagner double spherical-shell physical model (solid red line). The peak with a low amplitude at the low frequency is generated by the cell membranes, whereas the peak with a high amplitude at the high frequency is generated by the nuclear membranes. The curve has a double semi-circular shape, with a small arc at low frequency and a large arc at high frequency.

3.3. Impedance spectra of the bullfrog erythrocytes suspensions

Resistivity is a key indicator to measure the resistance characteristics of different substances. The resistivity is inversely proportional to the conductivity. The dielectric response characteristics of the bullfrog erythrocytes have never been investigated via the analysis of the trend of their electrical impedance spectra. Figure 5(a) shows the impedance spectra of the erythrocyte suspension: the resistivity (ρ) decreases with increase in the frequency (f). The values $\rho_{\rm l}$ and $\rho_{\rm h}$ correspond to the low- and high-frequency values of the resistivity, respectively. The resistivity increment ($\Delta\rho = \rho_{\rm l} - \rho_{\rm h}$) increases with increase in the Hct value, and the relation between $\Delta\rho$ and Hct is linear under $Hct < 0.4$ (Fig. 5(a)). The three-dimensional physical model fitting curve (solid line) of the impedance spectra provide the values of the resistivity of the cytoplasm (hemoglobin, $\rho_{\rm Hb}$) and the nuclear endoplasm ($\rho_{\rm np}$), which are (2.10 ± 0.35) Ω·m and (0.42 ± 0.10) Ω·m, respectively. The resistivity spectra of the cell membranes and the nuclear membranes are shown by the double peak curve with a tail warping in Figs. 5(c) and 5(d). The peak with a high amplitude at low frequency is generated by the cell membranes and it is a large arc, whereas the peak with a low amplitude at high frequency is generated by the nuclear membranes and is a small arc. They form a double semi-circular shape curve. With the further increase in frequency, the spectra exhibit a tail warping.

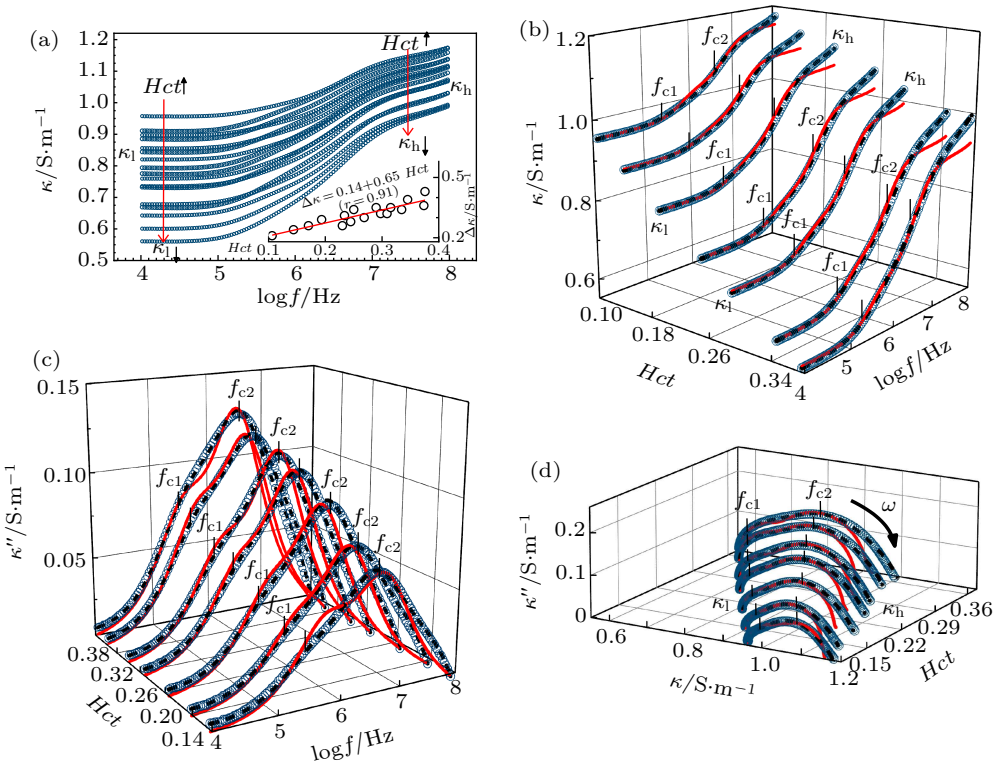

Fig. 4. Spectra of the real part [(a), (b)] and of the imaginary part (c) of the complex conductivity of the bullfrog erythrocytes suspensions and its complex planes (d). The hollow circle represents the experimental data, the dashed line is the Cole–Cole equation curve, and the solid line is the physical model curve based on the double spherical-shell model.

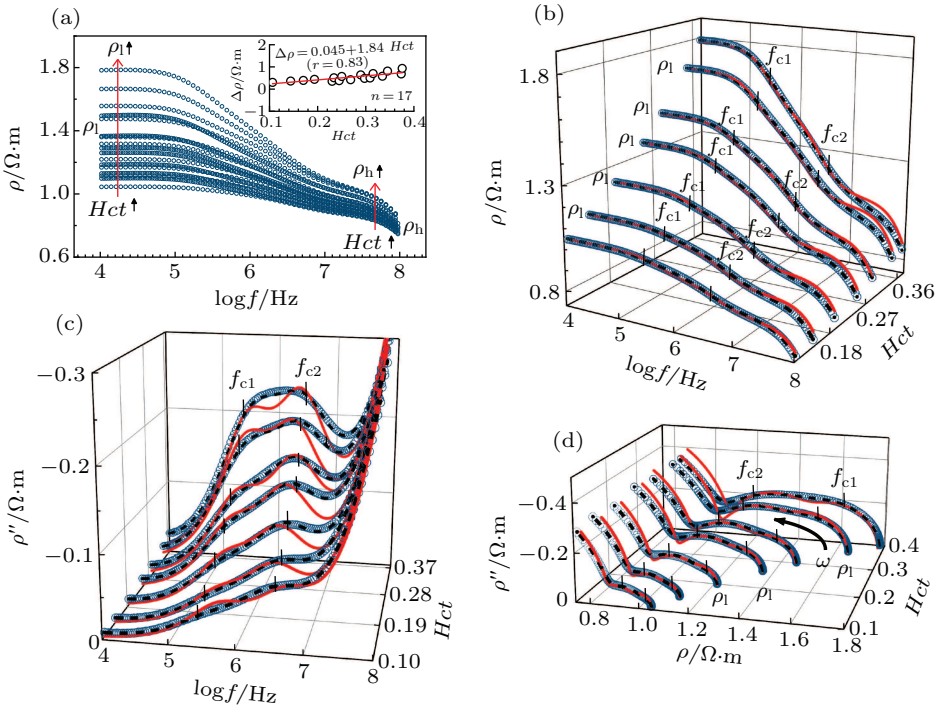

Fig. 5. Spectra of the real part [(a), (b)] and the imaginary part (c) of the complex resistivity of the bullfrog erythrocytes suspensions and its complex planes (d). The hollow circle represents the experimental data, the dashed line is the Cole–Cole equation curve, and the solid line is the physical model curve based on the double spherical-shell model.

3.4. Relation between the Haematocrit and the Cole–Cole equation parameters of the bullfrog erythrocytes

The relation between the Cole–Cole equation parameters and the *Hct* value of the 17 bullfrog erythrocytes suspensions (Fig. 6) was analyzed based on the correlation coefficient (r). The dielectric increment ($\Delta\varepsilon_1$ and $\Delta\varepsilon_2$) and the time distribution parameters (β_1 and β_2) exhibit a positive correlation with the *Hct* value (Figs. 6(a) and 6(d)). The values of ε_h and κ_l have a negative correlation with the *Hct* value (Figs. 6(c), 6(d)). The characteristic frequency parameters (f_{c1} and f_{c2})

and the m value ($m = 1.50$) are independent of any variation in Hct. Owing to the small slope value (0.09 and 0.02) of the time distribution parameters (β_1 and β_2), they have weakly affected by a change in Hct. In summary, the time distribution parameters (β_1, β_2), the characteristic frequencies (f_{c1} and f_{c2}), and the m values are independent of Hct. For this reason, they can be used as intrinsic electrophysiological parameters in the frequency domain of the erythrocytes. The characteristic frequencies enrich the electrophysiological indicators available to analyse the bullfrog erythrocytes. The calculated mathematical and double-spherical-shell physical model parameters of the bullfrog erythrocytes are given in Tables 1 and 2, respectively.

Table 1. Dielectric impedance spectra and parameters obtained via the Cole–Cole equation describing the mathematical model parameters of the bullfrog erythrocytes ($n = 17$).

Spectral parameters	Symbol/unit	Mean ± SD
Hematocrit	Hct	0.26 ± 0.08
The limiting permittivity at high frequencies	ε_h	72.59 ± 3.36
The limiting conductivity at low frequencies	κ_l/S·m^{-1}	0.77 ± 0.11
The first dielectric relaxation increment	$\Delta\varepsilon_1$	$(5.63 \pm 1.43) \times 10^3$
The second dielectric relaxation increment	$\Delta\varepsilon_2$	$(5.21 \pm 1.20) \times 10^2$
The first characteristic frequency	f_{c1}/kHz	297.06 ± 14.48
The second characteristic frequency	f_{c2}/MHz	3.73 ± 0.06
The first Cole–Cole parameter	β_1	0.86 ± 0.01
The second Cole–Cole parameter	β_2	0.98 ± 0.00
Constant	A	$(6.44 \pm 0.65) \times 10^9$
Power function power	m	1.50 ± 0.00
Residual	$R(\varepsilon + \kappa)$	0.38 ± 0.08

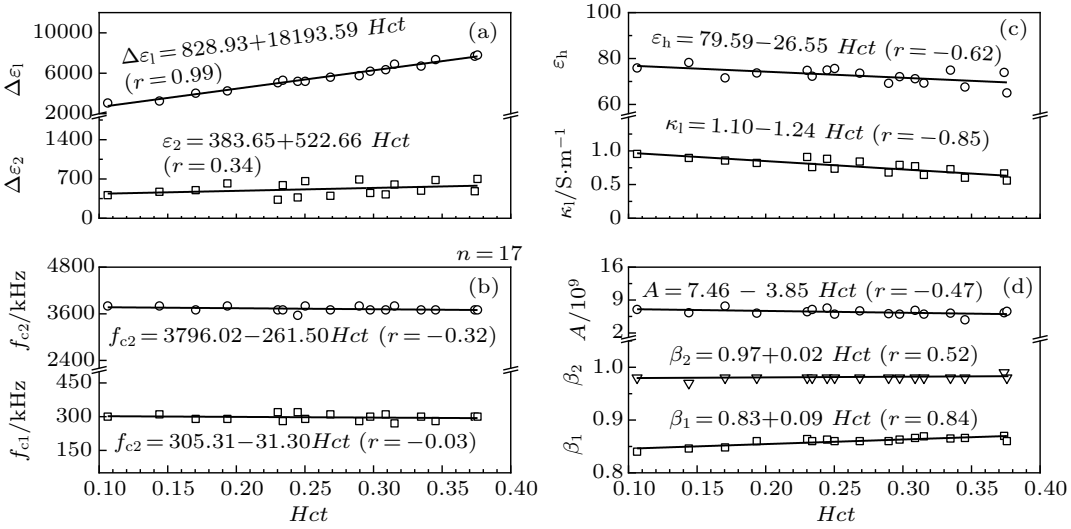

Fig. 6. Relation between the Cole–Cole equation parameters and the hematocrit (Hct) of the bullfrog erythrocytes.

Table 2. Dielectric impedance spectra and parameters obtained from the double spherical-shell physical model to describe the bullfrog erythrocytes ($n = 17$).

Phase parameters	Symbol/unit	Mean ± SD
Cell volume fraction	$Hct(\Phi)$	0.26 ± 0.08[b]
Extracellular fluid permittivity	ε_o	80.00
Extracellular fluid conductivity	κ_o/S·m^{-1}	1.18 ± 0.10
Extracellular fluid resistivity	ρ_o/Ω·m	0.85 ± 0.07
Cell membrane permittivity	ε_m	7.57 ± 0.38
Cell membrane conductivity	κ_m/S·m^{-1}	$1.00 \times 10^{-7} \pm 0.00$
Cell membrane resistivity	ρ_m/Ω·m	$1.00 \times 10^7 \pm 0.00$
Cytoplasmic permittivity	ε_{Hb}	60.00 ± 0.00
Cytoplasmic conductivity	κ_{Hb}/S·m^{-1}	0.50 ± 0.13
Cytoplasmic resistivity	ρ_{Hb}/Ω·m	2.10 ± 0.35
Cell nuclear membrane permittivity	ε_{ne}	23.59 ± 4.39
Cell nuclear membrane conductivity	κ_{ne}/S·m^{-1}	$1.00 \times 10^{-4} \pm 0.00$
Cell nuclear membrane resistivity	ρ_{ne}/Ω·m	$1.00 \times 10^4 \pm 0.00$
Nuclear endoplasmic permittivity	ε_{np}	60.00
Nuclear endoplasmic conductivity	κ_{np}/S·m^{-1}	2.56 ± 0.75
Nuclear endoplasmic resistivity	ρ_{np}/Ω·m	0.42 ± 0.10
Cell radius	R/μm	12.80[a]
Cell membrane thickness	d/nm	7.98 ± 0.05
Nuclear radius	R_n/μm	8.20 ± 0.32[c]
Cell nuclear membrane thickness	d_n/nm	40.00 ± 0.00
Cell membrane capacitance	C_m/μF·cm^{-2}	0.84 ± 0.04[d]
Nuclear membrane capacitance	C_{ne}/μF·cm^{-2}	0.52 ± 0.10[d]
Residual	$R(\varepsilon + \kappa)$	2.99 ± 0.43

[a]Optical microscopy; [b]hematocrit method;

[c]parameters from Plattner *et al.*;[25]; [d]$C_m = \varepsilon_{m\times}\varepsilon_v/d$, $C_{ne} = \varepsilon_{ne\times}\varepsilon_v/d_n$.

4. Discussion

In this paper, the dielectric properties of bullfrog nucleated erythrocytes were accurately analyzed via the double spherical-shell model. The spectra of their complex permittivity, complex conductivity, and complex resistivity as a function of the cell volume (10.63%–37.58%) were measured by using a precision impedance analyser. The erythrocytes exhibit a typical bimodal β-relaxation phenomenon in the frequency range of 10 kHz–110 MHz. By spectral analysis and several parameter extraction techniques, the low- and high-frequency characteristic parameters of the dispersion spectra and the Cole–Cole mathematical model parameters were obtained in low concentration conditions ($Hct < 0.4$). The permittivity (ε) gradually decreases with increase in the electric field frequency (f). With the increase in haematocrit (Hct), the low-frequency value of the permittivity ($\varepsilon_l = \varepsilon|_{f=77\ \text{kHz}}$) increases, whereas its high-frequency value ($\varepsilon_h = \varepsilon|_{f=95\ \text{MHz}}$) remains almost unchanged. Moreover, the dielectric increment ($\Delta\varepsilon$) shows a linear positive trend as a function of the Hct value [$\Delta\varepsilon = (1470.11 + 17117.81)\ Hct$]. Similarly, the resistivity (ρ) of the erythrocytes suspension decreases with

the increase in f; while the low-frequency value of the resistivity ($\rho_{\rm l} = \rho|_{f=10\ {\rm kHz}}$), the high-frequency value ($\rho_{\rm h} = \rho|_{f=100\ {\rm MHz}}$), and the resistivity increment ($\Delta\rho$) increase as a function of Hct. There is a weak linear correlation can be observed between $\Delta\rho$ and Hct. In addition, a change in Hct shows a limited effect on the time distribution parameters (β_1 and β_2). These results show that the low-frequency time distribution parameters (β_1, 0.86 ± 0.01), the high-frequency time distribution parameters (β_2, 0.98 ± 0.00), the low-frequency characteristic frequency [$f_{\rm c1}$, (297.06 ± 14.48) kHz], the high-frequency characteristic frequency [$f_{\rm c2}$, (3.73 ± 0.06) MHz], and the m value ($m = 1.50$) are intrinsic electrophysiological parameters, which can be used to fully characterize the bullfrog erythrocytes. When this data is compared with the characteristic parameters of the human plasma ($\varepsilon_{\rm p} = 78.00$, $\kappa_{\rm p} = 1.20$ S/m), cell membrane ($\varepsilon_{\rm m} = 13.11$, $\kappa_{\rm m} = 0.54 \times 10^{-7}$ S/m), and cytoplasm ($\varepsilon_{\rm c} = 67.18$, $\kappa_{\rm c} = 0.49$ S/m),[26] the dielectric parameters of the bullfrog erythrocytes obtained via the Cole–Cole and the double shell models lie in the same data range. This shows that the results of this study are reliable. In addition, a double spherical-shell physical model based on the Maxwell–Wagner equation was established to analyze the β-relaxation contributions of the cell membrane, cytoplasm, nuclear membrane, and nucleoplasm of the bullfrog erythrocytes. This method can also be used to quantify the structural phase parameters of the erythrocytes, such as their cell membrane thickness and nuclear ratio. By fitting the complex permittivity, complex conductivity, and complex resistivity spectra of the bullfrog erythrocytes via the double spherical-shell physical model, the results show that the physical model curve almost coincides with the mathematical model curve. This indicates that such an analysis method can accurately provide the morphological structure of the bullfrog erythrocytes. In the real part of the permittivity (ε') spectra as a function of the frequency (f) a single peak is present (Fig. 3(a)). The plot of the real part of the permittivity (ε') as a function of its imaginary part (ε'') exhibits a single feature when the haematocrit content varies (Fig. 3(d)). Moreover, the spectra of the imaginary part of the conductivity (κ'') as a function of the frequency (f) is a double-peak curve with a low-amplitude feature in the low-frequency range and a high-amplitude feature in the high-frequency zone (Fig. 4(c)). The plot of the real part of the conductivity (κ') as a function of its imaginary part (κ'') is a double semi-circular curve with a series of small arcs in the low-frequency region and several large arcs in the high-frequency one (Fig. 4(d)). The permittivity and the conductivity spectra indicate the non-uniform characteristics of the medium in which the erythrocytes are analysed (Figs. 3 and 4). The peaks at low and high frequencies were derived from the dielectric response to the external electric field of the cell membrane and the nuclear membrane, respectively.

The relation between the resistivity spectra of the bullfrog erythrocytes suspensions and the Hct value was investigated in this work for the first time. The 3D physical model fitting curve shows that the dielectric responses of the cell and nuclear membranes exhibit a double-peak profile with a high-amplitude feature in the low frequency region and a low-amplitude peak with a tail warping in the high-frequency zone. The trend of the resistivity is consistent with the dielectric parameters and the conductivity. This further explains the dielectric response of the cell and nuclear membranes to the external electric field. The internal structural parameters of the bullfrog erythrocytes were determined by fitting their curves and using the vector superposition of their physical models. The cell membrane capacitance ($C_{\rm m-frog} = 0.84\ \mu{\rm F\cdot cm^{-2}}$) and the nuclear membrane capacitance ($C_{\rm ne-chicken} = 0.52\ \mu{\rm F\cdot cm^{-2}}$) are slightly higher than the same values reported for chicken erythrocytes ($C_{\rm m-chicken} = 0.40\ \mu{\rm F\cdot cm^{-2}}$, $C_{\rm ne-chicken} = 0.45\ \mu{\rm F\cdot cm^{-2}}$)[8] and human erythrocytes ($C_{\rm m-human} = 0.80\ \mu{\rm F\cdot cm^{-2}}$).[26] They are of the same order of magnitude.

The cytoplasmic conductivity of frog erythrocytes [$\kappa_{\rm Hb-frog} = (0.50 \pm 0.13)$ S/m] is similar to that of chickens and humans ($\kappa_{\rm Hb-chicken} = 0.36$ S/m, $\kappa_{\rm Hb-human} = 0.49$ S/m). This suggests that there is no significant difference in the dielectric specificity of the erythrocyte hemoglobin obtained from different biological sources. In addition, these results were compared with the dielectric parameters of nucleated cells obtained from Chinese hamsters' ovary cells (CHO), T lymphocytes, lymphocytes, and monocytes. Their cytoplasmic conductivity is significantly different (0.42, 0.65, 0.32, 0.56 S/m)[22] and is half that of the adrenal chromaffin cells [$\kappa_{\rm cyto-cc} = (1.14 \pm 0.25)$ S/m].[23] One can speculate that the presence of tiny particles in the cytoplasm is the main reason for such a high conductivity. These results provide a guide to evaluate the dielectric properties and the heterogeneity differences among cells, including nuclei and organelles.

5. Conclusion

This work focused on quantifying the electrical properties of nucleated erythrocytes and providing a method for resolving dielectric spectra applicable to spherical nucleated cells for basic research and hematological biodiversity analysis. To that end, (i) the complex permittivity $\varepsilon^*(\omega)$ spectra, complex conductance $\kappa^*(\omega)$ spectra, and complex resistivity $\rho^*(\omega)$ spectra of bullfrog erythrocytes with different Hct were measured in the 10 kHz–110 MHz frequency range. (ii) Based on the curve-fitting analysis of the Cole–Cole equation, we determined that bullfrog erythrocytes have two dielectric relaxations. The Cole–Cole mathematical model parameters were extracted to clarify the spectral characteristics of frog erythrocytes and to explore the relationship between these parameters

and Hct. (iii) The first dielectric dispersion originates from the cell membrane and the second dielectric dispersion originates from the nuclear membrane, which are precisely explained by the numerical calculations of the double spherical shell dielectric theory model. (iv) The spectral and structural phase parameters of nucleated erythrocytes were successfully and accurately quantified using the proposed method to obtain relaxation behavior, passive electrical properties and cellular structural parameters of erythrocyte suspensions, including the cell membrane, cytoplasmic, nuclear membrane and nucleoplasm. Thus, this study sheds some light on the analysis of the intrinsic electrophysiological parameters, and provides the values of the parameters of each structural phase of the bullfrog erythrocytes. These findings can pave the way for novel research projects to understand frog haematology and for further applications of dielectric impedance spectroscopy.

References

[1] Zhbanov A and Yang S 2020 *IEEE Trans. Biomed. Eng.* **67** 2965
[2] Torquato S and Haslach H 2002 *Appl. Mech. Rev.* **55** B62
[3] Salahuddin S, O'Halloran M, Porter E, Farrugia L, Bonello J, Sammut C V and Wismayer P S 2017 *IEEE Trans. Dielect. Electr. Insul.* **24** 3283
[4] Ma Q, Watanabe M and Suzaki T 2003 *Chin. J. Biomed. Eng.* **22** 309
[5] Bielinska I 1987 *Phys. Med. Biol.* **32** 623
[6] Asami K, Takahashi Y and Takashima S 1989 *Biochim. Biophys. Acta* **1010** 49
[7] Asami K 2016 *J. Membrane Biol.* **249** 31
[8] Gimsa J, Titipornpun K, Stubbe M and Gimsa U 2018 *Electrophoresis* **39** 2253
[9] David M, Levy E, Feldman Y, Ben Ishai P, Zelig O, Yedgar S and Barshtein G 2017 *Physiol. Meas.* **38** 1335
[10] Schwan H P 1963 *Physical Techniques in Biological Research*, ed. Nastuk W L (New York: Acdemic) pp. 323–407
[11] Wolf M, Gulich R, Lunkenheimer P and Loidl A 2011 *Biochim. Biophys. Acta* **1810** 727
[12] Guo F, Yao C, Li C and Mi Y 2013 *Transactions of China Electrotechnical Society* **28** 182
[13] Cole K S and and Cole R H 1941 *J. Chem. Phys.* **9** 341
[14] Cole K S and Cole R H 1942 *J. Chem. Phys.* **10** 98
[15] Guan H L, Chen X R, Jiang T, Du H, Paramane A and Zhou H 2020 *Chin. Phys. B* **29** 075204
[16] Furhaj A S, Muhammad K, Muhammad S S, H M Noor ul H K A, Sameen A, Ayesha P, Jalil ur R, Muhammad A K and Zaheer A G 2019 *Chin. Phys. B* **28** 088701
[17] Montalvão M F and Malafaia G 2017 *Environ. Sci. Pollut. R.* **24** 23411
[18] Liu H, Shi F, Tang X, Zheng S, Kolb J and Yao C 2020 *Bioelectrochemistry* **135** 107570
[19] Yao C, Hu X, Li C, Yan M and Sun C 2008 *Conf. Proc. IEEE Eng. Med. Biol. Soc.* **2008** 1032
[20] Zhao K, Bai W and Mi H 2006 *Bioelectrochemistry* **69** 49
[21] Wagner K W 1914 *Archiv Für Elektrotechnik (Archive for Electrical Engineering)* **2** 371
[22] Salimi E, Braasch K, Butler M, Thomson D J and Bridges G E 2016 *Biomicrofluidics* **10** 014111
[23] Sabuncu A C, Stacey M, Craviso G L, Semenova N, Vernier P T, Leblanc N, Chatterjee I and Zaklit J 2018 *Bioelectrochemistry* **119** 84
[24] Stacey M W, Sabuncu A C and Beskok A 2014 *Biochim. Biophys. Acta* **1840** 146
[25] Plattner H, Artalejo A R and Neher E 1997 *J. Cell Biol.* **139** 1709
[26] Zhbanov A and Yang S 2017 *Anal. Methods-UK* **9** 3302